W. D. Grobman
A. J. Speth
T. H. P. Chang

Proximity Correction Enhancements for 1-μm Dense Circuits

The proximity effect in electron-beam lithography, which is due to electron scattering in the resist and wafer, results in nonuniform exposure and development for patterns in which the incident doses of all the shapes are the same. Correction for this effect has been accomplished in the past primarily by varying the incident doses of all the shapes in order to achieve an equal average resultant dose per unit area for all shapes. We show that in the case of dense circuits with linewidths of about 1 μm or smaller, two enhancements to the proximity correction technique can be easily implemented. One of these is a simple approach to shape breakup (partitioning) to enable dose correction to be applied nonuniformly within the original design shapes. The other technique is a new type of algorithm for forming subsets of the design to perform self-consistent dose correction. These two enhancements are applied to LSI chip data for dense circuits and are shown to permit fabrication of circuits which would be more difficult to process using the proximity correction techniques described previously, due to the particular geometries present in these circuit designs. We also show the application of step and repeat pattern recognition algorithms to compact the resulting data, and consequently to reduce the amount of data by an amount which is greater than the increase in the number of shapes caused by partitioning.

Introduction

IBM Vector Scan (VS) electron-beam (e-beam) systems have been used as the lithographic tools in several research programs involving silicon and bubble technologies [1-6]. These systems have been used either in a direct-write mode, in which the e-beam delineates patterns in resist films that coat working substrates, or in a mask-making mode. Considerable experience has thus been gained with VLSI exposures with minimum feature sizes in the range of dimensions of ≤ 1 μm. Previous publications have detailed the hardware and various control functions of the VS system and the methods used in preparing the source pattern data for the system's exposure format [7-9].

In this paper, we report several recently implemented enhancements in the areas of dose correction and pattern data preparation. Two benefits derived from these enhancements are an improvement in development uniformity for high-resolution patterns characterized by large area exposures separated by fine ($\leq$1-μm) resist gaps, and an increase in the efficiency of the computational procedures used in preparing pattern data. All of these enhancements relate to aspects of correcting for the proximity effect, a phenomenon resulting from electrons incident on a solid substrate being scattered or backscattered differentially from the surface or within the bulk [10-17]. Thus, a thin resist film on a solid substrate, when impacted by an e-beam of negligibly small dimensions, absorbs energy over a range that is related to the energy of the incident beam, the resist and its thickness, and the substrate material. The spatial distribution of this energy absorption within the resist film is three-dimensional but can be approximated as a superposition of two Gaussian functions of position away from the incident beam [13] (a long- and a short-ranged one), *e.g.*, as a point-spread function convolved with the incident beam profile. For 25-keV (4×10^{-15} J) exposures on Si substrates [16] and for 0.6 μm of resist and an incident beam diameter of 0.1

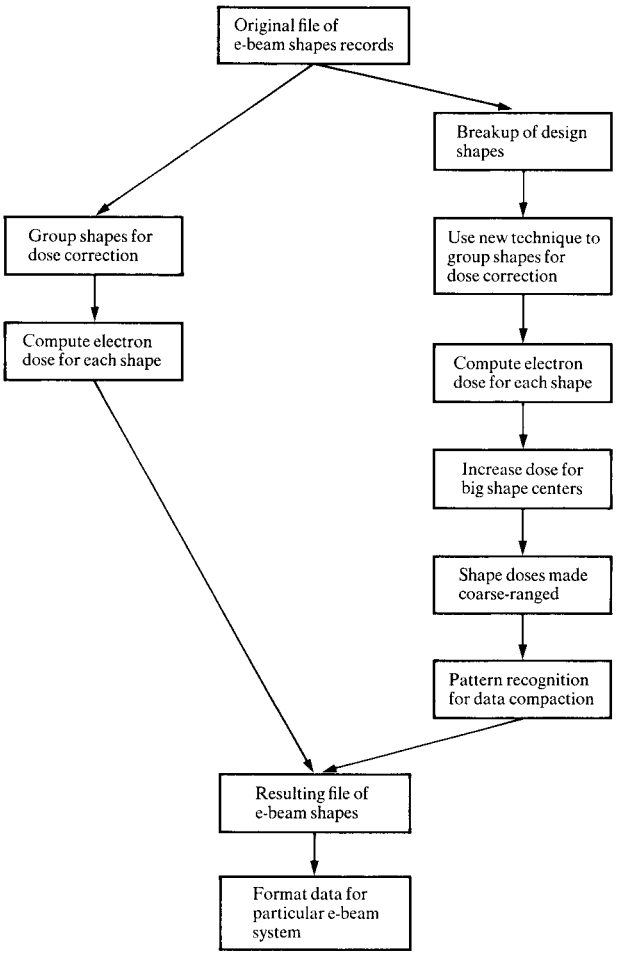

Figure 1 Data processing streams for dose correction scheme without partitioning [14c] (left-hand side) and with partitioning (current scheme; right-hand side).

μm, these Gaussian functions have halfwidths of $\approx$0.25 μm (short-range function α) and $\approx$2.5 μm (long-range function β). The short-range function α is very dependent on the e-beam diameter in the VS system and on the resist thickness. The value given here is only approximate. [*Editor's note*: α is equivalent to β_f, β to β_b, and η to η_E in the preceding paper by M. Parikh.]

The proximity effect has been widely considered in the literature [10–17] from two points of view: the description or measurement of the scattering function and the development of approaches for minimizing the practical consequences of the proximity effect. If a uniform electron dose is used to expose patterns, two commonly recognized consequences are that small isolated shapes receive a size-dependent dose and that neighboring pattern shapes may partially expose each other. The degree to which the resultant exposure distribution affects the surface topography of the developed resist is also related to the solubility (contrast) characteristics of the resist system being considered.

A widely recognized method for the compensation of proximity effects is to correct the incident dose of each shape in a pattern. A theory and computer algorithm called SPECTRE [14a, b] has been developed to compute these corrections in a self-consistent manner for vector-scan (VS) systems. This procedure adjusts the incident dose for each shape so that the resultant average exposure within the boundary of each shape is the same. In order to calculate the doses, shapes are first collected into groups (see left-hand side of Fig. 1). The individual shape doses are translated by the system's pattern generator into a clock frequency, which determines the scanning "fill-in" period for each shape. This procedure has had wide success in the correction of patterns comprised of small exposed regions in the resist (*e.g.*, bubble memory [6], FET circuits [4]). However, in the case of patterns requiring large exposed regions separated by small resist gaps, the enhancements described in this paper, modifications to the SPECTRE program, are quite important; they are summarized on the right side of Fig. 1. Both approaches operate on identical files of primitive shapes, each compatible in size and geometric type to VS system requirements. The left-hand path provides only for the adjustment of the exposure level of each input shape. The right-hand path performs some similar functions, but first breaks up ("partitions") many of the input shapes. In addition, the right-hand path contains a number of enhancements that allow the computation time to be significantly reduced compared to earlier software, as well as provide for compaction of the output data file and additional dose modification at the center of large shapes.

Enhancements for dense 1-μm circuits

• *Shape partitioning with increased dose at shape centers*

To date, most emphasis on the proximity effect problem has been directed toward correcting exposure levels of small shapes, *i.e.*, those whose smallest dimension is less than the size of the long-range (backscatter) Gaussian function. Shapes whose dimensions are in the range 0.5–2 μm would normally fit into this class. This approach has been reasonable since the experimental exposure and resist development process is normally tailored toward establishing dimensional fidelity of the smallest, and thus most critically sized, detail. However, the exposure distribution within large shapes varies strongly as a function of position, which compromises proper dose correction if the only degrees of freedom are the individual doses for

the original shapes. This deficiency becomes critical in cases where narrow gaps ($\lesssim 1$ μm) between large shapes are to be accurately delineated.

It has been found that improvements in resist development characteristics can be achieved by partitioning large shapes to better control the effective incident exposure profiles. Such an approach is sketched in Fig. 2, which shows a simple device consisting of two large shapes separated by a 1-μm gap. Figure 2(a) shows the original design version of this device, while Fig. 2(c) shows the device after partitioning. If proximity correction is applied to the two shapes in Fig. 2(a), the resultant dose near the gap is very different from that of the outer edges, as is shown for this shape printed in partially developed resist in Fig. 2(b). The partitioned design in Fig. 2(c) permits proximity correction to adjust the doses in these areas properly, leading to more uniform resist development as demonstrated in Fig. 2(d). Without this simple change in the design, the device is very difficult (or impossible) to process properly. A similar partitioning approach has been developed separately and independently [15].

Figures 3(a)-(d) illustrate the somewhat more general case of a 6-μm-wide line separated by 1 μm from a 1-μm line. Using the same scattering parameters as for Figs. 2(b) and (d) but with $\alpha = 0.33$ μm, absorbed energy distributions are shown for four distinct situations. Each case also shows a resist solubility distribution. The latter assumes a positive resist and an exposure level for which the solubility-exposure relationship is a square law. This condition is often close to the practical case [16, 17].

Figure 3(a) shows these distributions for the case in which the lines receive the same incident dose per unit area (no dose correction). Here, it is apparent that the 6-μm line will "develop out" well before the 1-μm line. Figure 3(b) shows the result of applying proximity correction without pattern partitioning. The correction increases the incident dose of the narrow line relative to that of the wide line. The facility for tight dimensional control of the narrow line's width is lost because of the continued development required to fully develop the edges of the 6-μm line. In Fig. 3(c), the wide line is partitioned with 1-μm borders, and then the usual dose correction program is applied. The dose in the edge region of the wide line is now uniform and nominally equal to that of the narrow line. Thus, all edges develop at approximately the same rate. However, although the most critical part of the pattern (the edges) is successfully treated, the development of the edges of the center of the wide line (dips in dose *vs.* x at about 1.3 and 4.6 μm) governs the development time, since only the *average* of this shape is correct. This problem substantially narrows the development process window because additional development of the pattern required to remove all resist in this region results in overdevelopment of the edges of the shape.

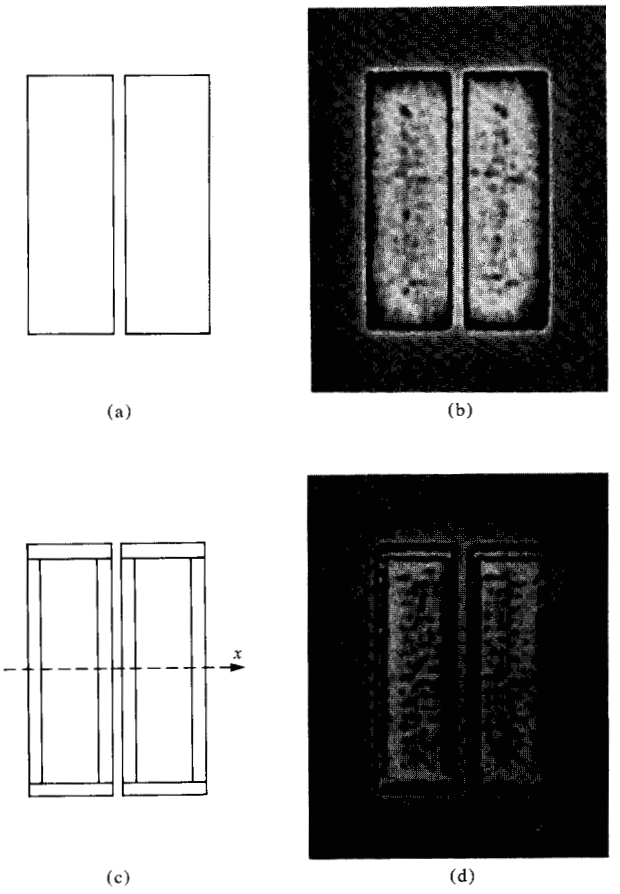

Figure 2 (a) Device in which two large exposed regions define a narrow ($\lesssim$1-μm) resist gap. (b) Photograph showing the partially developed resist for this unpartitioned case. (c) Same device design, but partitioned according to the scheme of the present paper. This permits the dose correction scheme of Ref. [14c] to more uniformly tailor the dose received by the resist. (d) Photograph showing the partially developed resist for this partitioned case.

Finally, in Fig. 3(d) we artificially "override" by 15% the calculated dose-corrected value for the exposure of the central region. Both the edge region and the central area of the large stripe are now seen to have a relatively uniform exposure and thus "develop out" uniformly. Control of the development time can thus be determined by the most critical features, the fine detail.

This approach is now used in processing all patterns. Any rectangular shape whose x and y dimensions both exceed some threshold width (presently 2 μm) is broken

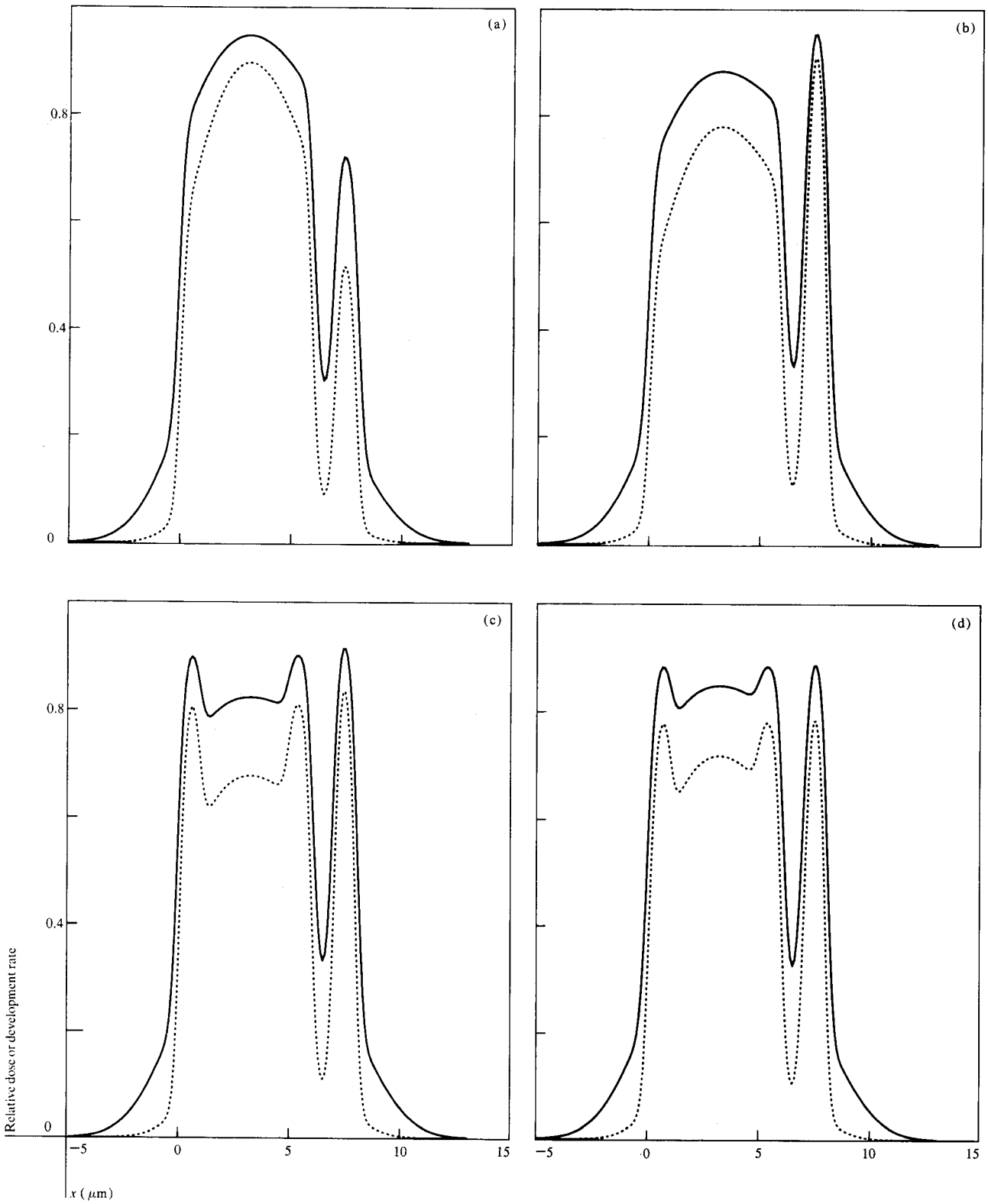

Figure 3 Resultant dose *vs.* position (solid lines) and resist development rate *vs.* position (dashed lines) for the case of two lines in the y direction (a 6- and a 1-μm line) separated by 1 μm. The electron scattering parameters used [16] were $\alpha = 0.33$ μm, $\beta = 2.35$ μm, $\eta = 0.86$ μm. (η is the ratio of the deposited energies from the short-range and long-range components.) (a) Case where dose is uncorrected; (b) dose correction of the original design; (c) dose correction after partitioning; and (d) dose correction after partitioning, but with the center shape given 1.15 times the nominal dose.

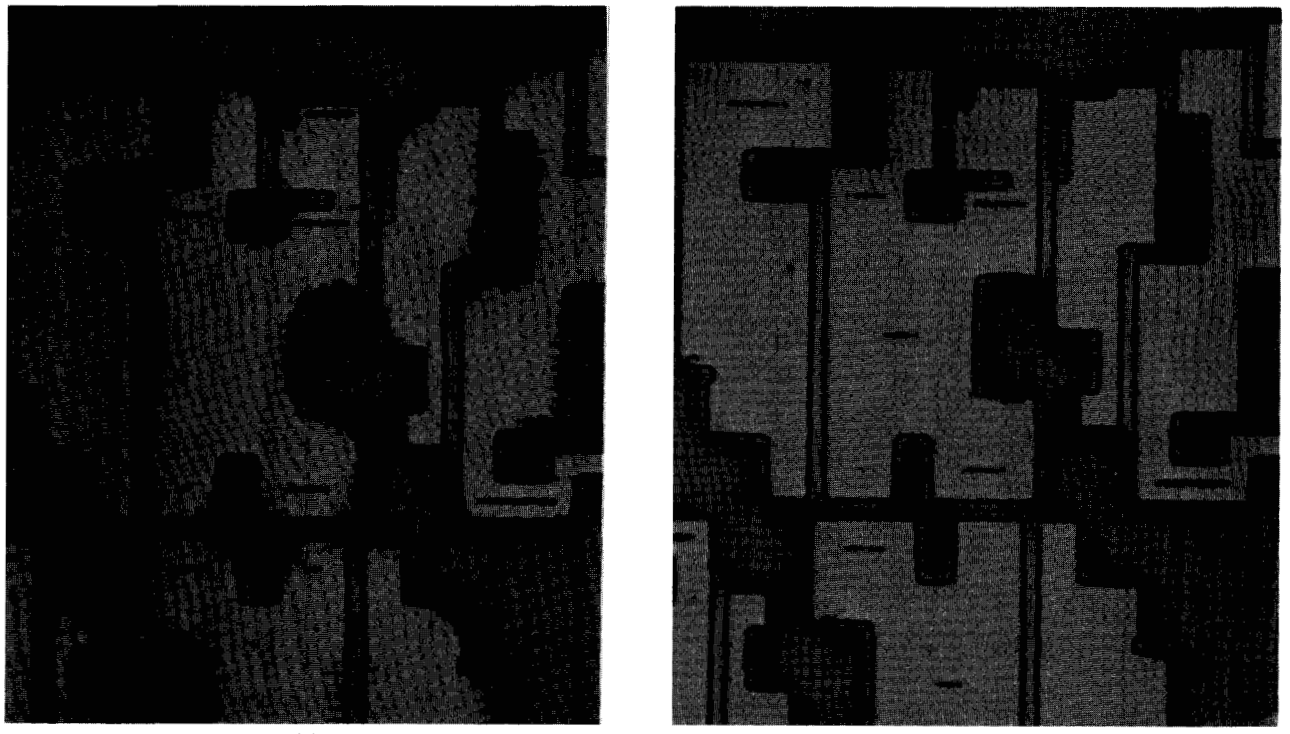

(a) (b)

Figure 4 A partially developed dense pattern after dose correction, but without partitioning. The smallest pattern feature (gap) is 1 μm. (b) The same design as in (a), but with partitioning done before dose correction and with the centers of the partitioned shapes given a dose 1.15 times that of the base dose.

into four perimeter shapes of 1-μm width and one central shape. Shapes with x or y dimensions <2 μm are not altered. After dose correction, shapes which are >2 μm in both dimensions are recognized to be "center" shapes, and their doses are replaced by 1.15 times the nominal dose (see Fig. 1).

For dense circuits, this partitioning approach is quite successful in producing uniform development, which is the key to successful processing. Figure 4 demonstrates this point. Resist patterns that are almost totally developed are shown both for the case of non-partitioned and partitioned patterns. In these circuits, dose correction has been applied in the same manner to both patterns. These patterns demonstrate the utility of partitioning in achieving uniform resist development at the edges of shapes, which are the most critical areas. These patterns also show the importance of breaking up shapes before dose correction for significant classes of circuit patterns.

• *New proximity correction shape-grouping algorithm*

Another enhancement we have made is in the portion of the dose correction technique that groups patterns into subfields to improve the efficiency of the computation of doses. Figures 5(a)–(c) illustrate aspects of the scheme used in Ref. [14c], while Fig. 5(d) illustrates our technique. Figure 5(a) is a schematic representation of a small portion of a chip in which there are areas densely populated with small shapes (*e.g.*, memory arrays) as well as areas in which long shapes predominate (*e.g.*, support circuits). In order to calculate the self-consistent proximity effect of all the shapes on one another, shapes belonging to "subzones" of the chip are grouped together and then the interactions among all the shapes in each subzone are calculated. As is indicated in Fig. 5(a), subzones are defined by an arbitrary coarse grid on top of the design, and shapes are defined to belong to a subzone if the lower left corner of the shape is within the subzone. Two typical subzones (labeled I, J and I', J') are shown with shapes belonging to them shaded. Before calculating the effects of all the shapes in a subzone on one another, it is important to consider the effects of shapes not belonging to the subzone of current interest but having an effect on its shapes.

Figure 5(b) shows the implementation of Ref. [14c] for including such neighboring shapes. A frame is drawn around a subzone of interest and shapes not in the subzone but having a vertex within the frame are included in

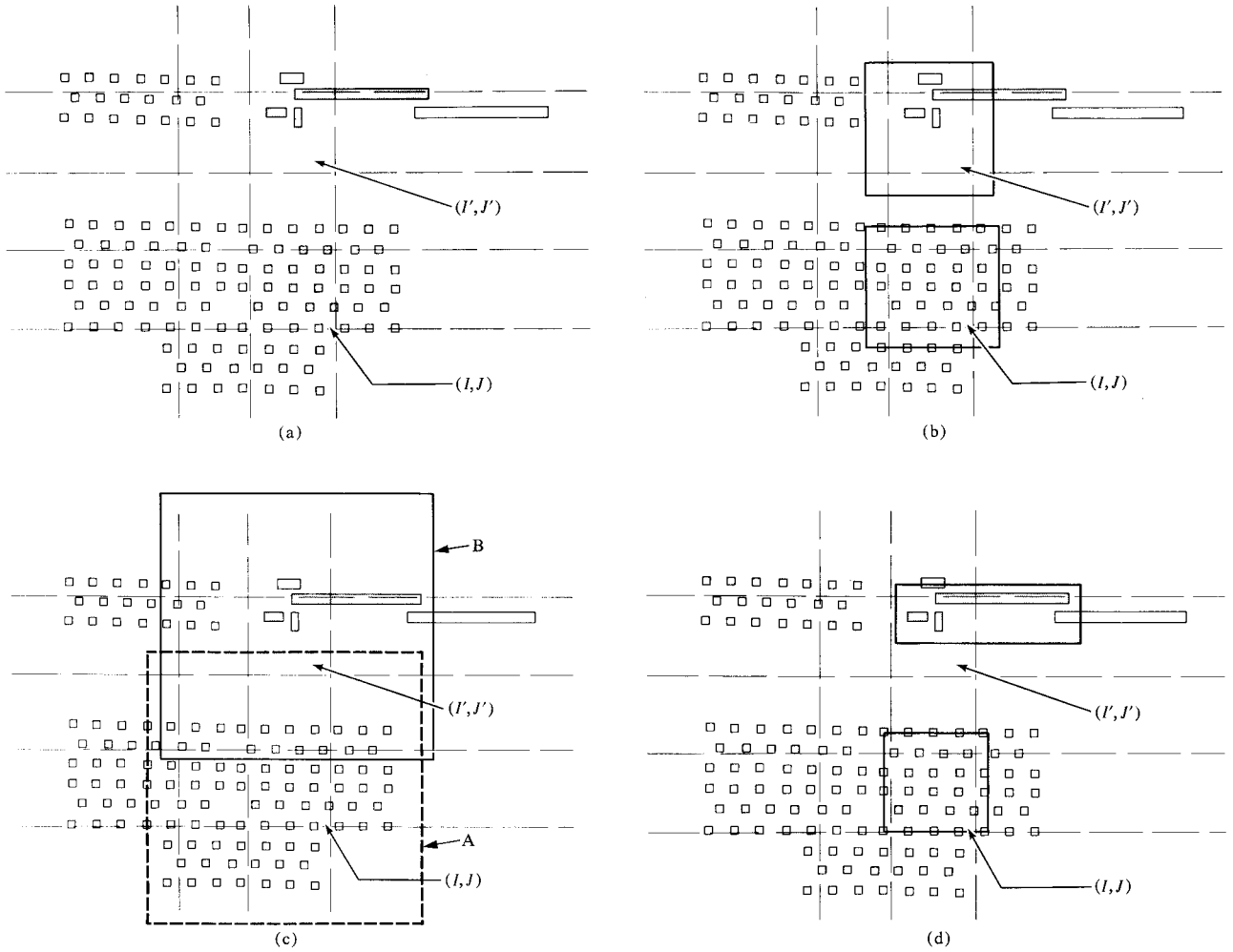

Figure 5 (a) A pattern containing both dense groups of small shapes and sparse long lines. The dashed lines divide the design into subzones, and shapes belonging to the (I', J') and (I, J) subzones are shaded. (b) Frames are drawn around subzones but are not large enough to include the influence of all shapes on subzone shapes. (c) Larger frames (A and B) cure the problem of incorporating all of the proper shape-shape effects, but incorporate too many unnecessary shapes. (Frame A has been displaced for clarity.) (d) The technique of the present paper uses frames that permit shapes in a given subzone to interact with fewer shapes than in 5(c), but in such a manner as to include all interactions properly.

the calculation. The frame size is the same for every subzone in the chip, and is an input parameter to the computer program. For the frame size shown, the dense pattern of small shapes in subzone (I, J) has neighboring shapes properly accounted for in calculating the doses; however, the (I', J') subzone has one long shape that extends far outside of the frame associated with it. The interaction of this shape with others thus cannot be properly calculated.

Figure 5(c) shows a solution to this problem achieved by simply changing the frame dimensions to very large ones. Then, long shapes extending far from their subzone can have their dose properly calculated. However, this approach suffers the serious disadvantage that its central processing unit (CPU) time efficiency is low. The enlargement of the frame dimension incorporates many shapes that often have no effect on the shapes of interest into the calculation of the (I', J') subzone shape doses. In dense memory areas this approach has brought a great many more shapes into the calculation and many of these are not required at all. In attempting to properly calculate the doses for subzone (I', J') in this example, one has unnecessarily increased the size of the (I, J) subzone calculation by a large factor.

We have developed a new algorithm for incorporating shapes associated with those in a particular subzone. In the shape-grouping step of the calculation, we first find all the shapes in a particular subzone and then generate for each subzone a frame that is tailored to the requirements of the shapes it contains; see Fig. 5(d). The frame has

been constructed so that it is the smallest rectangle that includes all of the shapes of the subzone of interest. This rectangle is expanded slightly beyond the range of the proximity effect (typically ≈ 5 μm). This technique properly calculates the effect of neighboring shapes belonging to a particular subzone in a manner independent of other subzones. In this way, CPU time is decreased while the effects of all shapes on one another are properly calculated. The implementation of this new algorithm has been instrumental in reducing CPU time for large-chip post-processing. It also prevents errors which the original scheme makes if improper subzone and frame sizes are chosen when running the dose correction program.

- *Dose "blurring" and data compaction*

One additional data manipulation has been used to compact the data (see Fig. 1) and thereby reduce the size of the data set produced by the partitioning software. A great deal of the data for dense circuits can be represented as regular rectangular repeats of a given shape ("step and repeats" of the shape). In the VS systems, the pattern generator [18, 19] contains circuits that can accept a step-and-repeat command and execute a subsequent e-beam write of a step-and-repeat pattern. By using software that recognizes step-and-repeated shapes in the pattern data flow, the final circuit data, formatted for the VS e-beam machine, can be greatly compacted. This procedure is discussed in detail in Ref. [19].

This approach has been applied to partitioned circuits written on the VS system and has resulted in a factor of two to four data-volume improvement. However, to ensure significant compaction, the doses resulting from proximity correction (which calculates doses to 1 part in 1000 precision) must be made more coarse-ranged. This step is required so that large blocks of shapes that differ only slightly in dose can be treated as having the same final written dose, thus permitting the step-and-repeat pattern recognition technique [19] to be used to obtain significant compaction. This "blurring" of shape doses is done in such a way that dose steps are of the order of a few percent. This is still fine enough so that proximity correction is properly implemented but is coarse enough to permit significant data compaction to be achieved.

Summary

We have described here two changes for improving proximity correction calculations. One of these is a simple technique for breaking up individual shapes before dose correction, in order to permit dose correction to more flexibly tailor dose *vs.* position. Such an approach is especially needed in the case in which fine resist features are to remain, separating larger exposed areas. However, this technique is not important for circuits produced from the exposure of small individual devices [4, 6], but it is needed in other types of patterns such as those in which subtractive etching is used rather than lift-off or plating. This approach may, however, lead to a significant increase in the size of the pattern data set. There are potentially more sophisticated algorithms which "look for" areas requiring partitioning, based on a calculation of geometrical areas that would benefit from shape breakup [20]. However, such shape-shape interaction calculations are lengthy. The simple scheme presented here is thus an attractive alternate approach to this problem.

We have also presented here for the first time a new approach to grouping shapes prior to dose corrections. This approach is potentially more efficient in CPU time than previously reported schemes and is not subject to errors caused by a choice of parameters which do not fit properly with a particular design.

Finally, we have made these changes along with others which further improve dose distribution and compact the resulting data. These new approaches to proximity effect correction not only increase the ease with which resist is processed, but also improve the linewidth control.

Acknowledgments

The technical assistance of K. Murphy, T. Donohue, H. Luhn, J. Powers, and H. Voelker is gratefully acknowledged. We have had useful discussions with many people including B. Crowder, C. Osburn, and T. W. Studwell.

References

1. H. N. Yu, R. H. Dennard, T. H. P. Chang, C. M. Osburn, V. DiLonardo, and H. E. Luhn, "Fabrication of a Miniature 8K-bit Memory Chip using Electron Beam Exposure," *J. Vac. Sci. Technol.* **12,** 1297 (1975).
2. H. N. Yu, A. Reisman, C. M. Osburn, and D. L. Critchlow, "1 Micron MOSFET VLSI Technology: Part I—An Overview," *IEEE J. Solid-State Circuits* **SC-14,** 240 (1979).
3. W. R. Hunter, L. Ephrath, W. D. Grobman, C. M. Osburn, B. L. Crowder, A. Cramer, and H. E. Luhn, "1 Micron MOSFET VLSI Technology: Part V—A Single-Level Polysilicon Technology Using Electron Beam Lithography," *IEEE J. Solid-State Circuits* **SC-14,** 240 (1979).
4. W. D. Grobman, H. E. Luhn, T. P. Donohue, A. J. Speth, A. Wilson, M. Hatzakis, and T. H. P. Chang, "1 μm MOSFET VLSI Technology: Part VI—Electron Beam Lithography," *IEEE J. Solid-State Circuits* **SC-14,** 282 (1979) and *IEEE Trans. Electron Devices* **ED-26,** 360 (1979).
5. T. H. P. Chang, M. Hatzakis, A. D. Wilson, A. J. Speth, A. Kern, and H. Luhn, "Scanning Electron Beam Lithography for Fabrication of Magnetic Bubble Circuits," *IBM J. Res. Develop.* **20,** 376 (1976).
6. D. C. Hofer, J. V. Powers, and W. D. Grobman, "X-Ray Lithographic Patterning of Magnetic Bubble Devices with Submicron Dimensions," *Proceedings of the Fifteenth Symposium on Electron, Ion, and Laser Beam Technology*, Boston, MA, May 29-June 1, 1979; T. H. P. Chang, Ed., American Vacuum Society, American Institute of Physics, New York, to be published.

7. A. J. Speth, A. D. Wilson, A. Kern, and T. H. P. Chang, "Electron Beam Lithography using Vector Scan Techniques," *J. Vac. Sci. Technol.* **12,** 1235 (1975).
8. T. H. P. Chang, A. D. Wilson, A. J. Speth, and C. H. Ting, "Vector Scan I: An Automated Electron Beam System for High Resolution Lithography," *Proceedings of the Seventh International Conference on Electron and Ion Beam Science and Technology*, Washington, DC, May 1976; R. Bakish, Ed., The Electrochemical Society, Princeton, NJ, 1976, p. 392.
9. T. H. P. Chang, A. J. Speth, C. H. Ting, R. Viswanathan, M. Parikh, and E. Munro, "The Probe Forming and Deflection System for the Vector Scan I E/B Lithography System," Ref. [8], *loc. cit.*, p. 377.
10. T. O. Sedgwick, A. N. Broers, and B. J. Agule, "A Novel Method for Fabrication of Ultra-Fine Metal Lines by Electron Beams," *J. Electrochem. Soc.* **119,** 1769 (1972).
11. J. S. Greeneich and T. Van Duzer, "An Exposure Model for Electron Sensitive Resists," *IEEE Trans. Electron Devices* **ED-21,** 286 (1974).
12. D. F. Kyser and K. Murata, "Monte Carlo Simulation of Electron Beam Scattering and Energy Loss in Thin Films on Thick Substrates," *Proceedings of the Sixth International Conference on Electron and Ion Beam Science and Technology*, San Francisco, CA, 1974; R. Bakish, Ed., The Electrochemical Society, Princeton, NJ, p. 205.
13. T. H. P. Chang, "Proximity Effect in Electron Beam Lithography," *J. Vac. Sci. Technol.* **12,** 1271 (1975).
14. Mihir Parikh, (a) "SPECTRE—A Self-Consistent Proximity Effect Correction Technique for Resist Exposure," *J. Vac. Sci. Technol.* **15,** 931 (1978); (b) "Corrections to Proximity Effects in Electron Beam Lithography. I. Theory, (c) II. Implementation, (d) III. Experiment," *J. Appl. Phys.* **50,** 4371, 4378, 4383 (1979); (e) "Proximity Effects in Electron Lithography: Magnitude and Correction Techniques," *IBM J. Res. Develop.* **24,** 438 (1980).
15. J. H. C. Phang and H. Ahmed, "A New Proximity Effect Correction Method for Accurate Pattern Fidelity," *Proceedings of Microcircuit Engineering '79*, September 1979, Institute of Semiconductor Electronics, Aachen, Germany, to be published.
16. W. D. Grobman and A. J. Speth, "An Exposure Wedge for Electron Beam Lithography Development Control and for the Determination of Resist Development and Proximity Parameters," *Proceedings of the Eighth International Conference on Electron and Ion Beam Science and Technology*, Seattle, WA, May 1978; R. Bakish, Ed., The Electrochemical Society, Princeton, NJ, p. 276.
17. A. R. Neureuther, D. F. Kyser, K. Murata, and C. H. Ting, "Electron Beam Resist Line Edge Profile Modeling," Ref. [16], *loc. cit.*, p. 265.
18. A. M. Patlach, P. R. Jaskar, and T. W. Studwell, "Electron Beam Lithographic Pattern Generation System," *Proceedings of the Fourteenth Symposium on Electron, Ion, and Laser Beam Technology*, Palo Alto, CA, May 1977; G. L. Varnell and J. L. Bartelt, Eds., American Vacuum Society, American Institute of Physics, New York. See also *J. Vac. Sci. Technol.* **15,** 874 (1978).
19. W. D. Grobman and T. W. Studwell, "Data Compaction and Vector Scan Electron Beam System Performance Improvements using a Novel Algorithm for Recognition of Pattern Step and Repeats," Ref. [6], *loc. cit.*
20. T. P. Chang, W. D. Grobman, and A. J. Speth, "Partitioning E-Beam Data for Proximity Corrections," *IBM Tech. Disclosure Bull.* **20,** 3809 (1978).

Received January 16, 1980; revised February 14, 1980

The authors are located at the IBM Thomas J. Watson Research Center, Yorktown Heights, New York 10598.